Enhancement of self-energy effects of phonons with finite wave vectors due to Fermi-surface nesting

F. Marsiglio
Theoretical Physics Branch, AECL Research, Chalk River Laboratories, Chalk River, Ontario, Canada K0J 1J0
(Received 13 August 1992)

The changes in phonon self-energy due to superconductivity are investigated for all wave vectors in the Brillouin zone, for two types of gap-function symmetry (s or d wave). We also study the phonon self-energy as a function of frequency, and for various electron concentrations. We adopt a simple tight-binding model that includes the important feature of a nested Fermi surface at half-filling. The changes in phonon self-energy arise from electron-phonon coupling. However, we make no assumption regarding the mechanism giving rise to superconductivity. We present possible signatures of an s- or d-wave gap function observable through inelastic-neutron-scattering experiments. Observation of any of these features in the high-T_c oxides would assist greatly in clarifying the gap function and Fermi-surface topology in these compounds.

I. INTRODUCTION

In the past few years there have been many indications that a sizeable electron-phonon coupling is present in many of the high-T_c oxides.[1] In the bismuthates, conventional indicators, such as tunneling and isotope measurements, have strongly suggested that the electron-phonon interaction is involved in the superconductivity in these compounds. In the cuprates, however, the isotope coefficient is generally anomalously low, and while structure is present in some tunneling experiments, its origin is not understood.

Nonetheless, even in the cuprates, Raman scattering,[2] neutron absorption spectroscopy,[3] infrared spectroscopy,[4] and ion channeling[5] experiments have all indicated that a large electron-phonon coupling exists in these materials. On the theoretical side, Zeyher and Zwicknagl[6] have been able to interpret many of the $\mathbf{q}=0$ phonon shifts and broadenings observed with Raman spectroscopy, through an Eliashberg formulation of the phonon self-energy. Marsiglio, Akis, and Carbotte[7] have extended this work by using a real axis formulation, and have obtained a phonon narrowing in the superconducting state with the addition of impurities, in agreement with observation.[8]

In the meantime, neutron spectroscopy and ion channeling experimental results have been interpreted to indicate a large electron-phonon coupling. Zeyher[9] has thus calculated the change in the phonon self-energy at $q\neq 0$, assuming a quasi-two-dimensional Fermi surface (a cylinder). He found that the calculated phonon changes due to superconductivity at large $\mathbf{q}$ are too small to account for the changes reported in Refs. 3 and 5. The purpose of this paper is to re-address this question in the following way: We will assume a two-dimensional tight-binding model, so that near half-filling the Fermi surface is nearly nested. Phonons with momentum vectors close to the nesting vector are then expected to undergo large changes in frequency and linewidth as the material goes superconducting, comparable to those for $\mathbf{q}=0$ phonons. In fact, neutron-scattering experiments, which probe directly these momentum transfers, should detect large frequency and linewidth changes in the superconducting state. Ruvalds *et al.*[10] have already argued that sufficient evidence exists from neutron-scattering and other measurements in the normal state that the Fermi surface in the cuprates is highly nested.

In addition, there is an increasing body of evidence that the gap function in the cuprates may not have s-wave symmetry, as initially thought.[11] Hence, we will investigate the expected changes in phonon frequencies and linewidths due to superconductivity with a gap function of d-wave symmetry, in addition to one with s-wave symmetry. Sufficiently accurate inelastic-neutron-scattering measurements could in principle distinguish between the two possible symmetries. In the past such measurements were successfully carried out by Axe and Shirane[12] and coworkers on Nb_3Sn and Nb. More recently Chou *et al.*[13] conducted the same experiment on a $La_{1.85}Sr_{0.15}CuO_4$ single crystal, and observed no change in the phonon linewidths due to superconductivity. However, their measurements, while carried out along the (110) direction, did not approach the zone boundary. Moreover, while phonon changes have been observed by many groups using Raman scattering in the $YBa_2Cu_3O_{7-\delta}$ compound, none have been reported for $La_{1.85}Sr_{0.15}CuO_4$, and $YBa_2Cu_3O_{7-\delta}$ may be a better candidate for study. Indeed, a preliminary observation of a frequency change due to superconductivity has been reported by Reichardt.[14]

The outline of the paper is as follows: In Sec. II we summarize the theory used and point out some of its limitations. In Sec. III we provide results as a function of phonon momentum $\mathbf{q}$, energy ν, and electron chemical potential μ, which, for our simple band structure, determines the Fermi surface. A summary is provided in the

final section. A short report of this work was given at the Sante Fe conference.[15] More recently, Flatté[16] has presented similar ideas. We should also add that the underlying assumption in this work is that the electronic structure is described by a single band near half-filling. Certainly other hypotheses exist,[17] where the effects described here will not occur. Moreover, it should be kept in mind that we postulate an electron-phonon coupling to give the phonon self-energy effects, but this does not necessarily imply that the electron-phonon mechanism drives superconductivity.

II. THEORY

We adopt the simplest approximation to the phonon self-energy which, in the normal state, amounts to evaluating the charge susceptibility:

$$\chi(\mathbf{q},i\nu_n)=-\frac{1}{2}\int_0^\beta d\tau e^{i\nu_n\tau}\langle\Omega|\rho(\mathbf{q},\tau)\rho(-\mathbf{q},0)|\Omega\rangle\ , \tag{1}$$

where

$$\rho(\mathbf{q},\tau)=\frac{1}{\sqrt{N}}\sum_{k\sigma}c^\dagger_{k+q,\sigma}(\tau)c_{k,\sigma}(\tau)\ , \tag{2}$$

and $|\Omega\rangle$ is the ground-state wave function. Here $c^\dagger_{k,\sigma}(\tau)$ is the creation operator for an electron with momentum $\mathbf{k}$ and spin σ at imaginary time τ. The charge susceptibility is given at wave vector $\mathbf{q}$ and Matsubara frequency, $i\nu_n$ ($\equiv i2\pi Tn$, n an integer). In the superconducting state, $|\Omega\rangle$ is the BCS superconducting ground state, and Eq. (1) is evaluated by using the Bogoliubov-Valatin transformation. Upon evaluation the susceptibility is analytically continued to real frequencies $[\chi(\mathbf{q},i\nu_n)\rightarrow\chi(\mathbf{q},\nu+i\delta)]$. The phonon self-energy, $\Pi(\mathbf{q},\nu+i\delta)$, is then proportional to the susceptibility

$$\Pi(\mathbf{q},\nu+i\delta)=|g|^2\chi(\mathbf{q},\nu+i\delta)\ , \tag{3}$$

where g is the electron-phonon coupling constant, which we have assumed is structureless in momentum. Hereafter, we confine ourselves to a study of $\chi(\mathbf{q},\nu+i\delta)$. The end result, in the superconducting state, is

$$\chi(q,\nu+i\delta)=\frac{1}{2N}\sum_k\left\{a_+(k,q)[f(E_k)-f(E_{k+q})]\left[\frac{1}{\nu+i\delta+E_k-E_{k+q}}-\frac{1}{\nu+i\delta-(E_k-E_{k+q})}\right]\right.$$
$$\left.+a_-(k,q)[1-f(E_k)-f(E_{k+q})]\left[\frac{1}{\nu+i\delta-(E_k+E_{k+q})}-\frac{1}{\nu+i\delta+(E_k+E_{k+q})}\right]\right\}\ , \tag{4}$$

where $E_k\equiv\sqrt{(\epsilon_k-\mu)^2+\Delta_k^2}$, $f(E_k)$ is the Fermi function, and $a_\pm(k,q)$ are the so-called coherence factors:

$$a_\pm(k,q)=1\pm\frac{(\epsilon_k-\mu)(\epsilon_{k+q}-\mu)-\Delta_k\Delta_{k+q}}{E_kE_{k+q}}\ . \tag{5}$$

Vector symbols have been suppressed for clarity. The chemical potential μ determines the number of electrons in the system. Finally, Δ_k is the gap function. For our purposes, we take Δ_k as given, with either s-wave or d-wave symmetry;

$$\Delta_k=\begin{cases}\Delta_0, & s\text{ wave}\\ (\Delta_0/2)(\cos k_x-\cos k_y), & d\text{ wave}\ ,\end{cases} \tag{6}$$

where Δ_0 is the maximum value of the gap function. The d-wave form has nodes at points on the Fermi surface. Here we are assuming that the important effects are in two dimensions. The band structure that we will assume in the remainder of the paper arises from nearest-neighbor overlaps only, $\epsilon_k=-2t(\cos k_x+\cos k_y)$, and has the important property that the Fermi surface is nested at half-filling. As already mentioned, there is some evidence that the Fermi surface is nested in the cuprates, and while the actual band structure will differ significantly from the one we are using, it is not our purpose here to try to quantitatively predict the phonon self-energy effects in these compounds; rather we wish to investigate qualitative effects which will arise due to nesting in the simplest possible model.

To understand the qualitative difference between results for a gap with s- or d-wave symmetry, we show in Fig. 1 the single-particle density of states, $g(E)$ vs E for the normal state, superconducting state with s-wave gap function, and the superconducting state with d-wave gap functions. The analytic expressions are given here for reference. In the normal state,

$$g_n(\epsilon)\equiv(1/2\pi^2t)K[1-(\epsilon/4t)^2]\ . \tag{7a}$$

In the superconducting state, at half-filling, the result with an s-wave gap function is

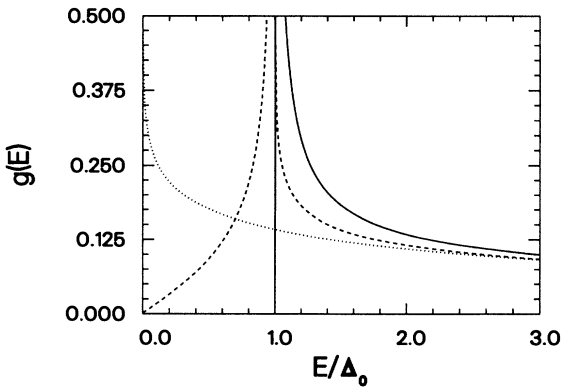

FIG. 1. Density of electron states $g(E)$ vs E/Δ_0 for the nearest-neighbor tight-binding model, at half-filling, for the normal state (· · · ·), the s-wave superconducting state (——), and the d-wave superconducting state (— — —).

$$g_s^s(E)\equiv\frac{|E|}{\sqrt{E^2-\Delta_0^2}}g_n(\sqrt{E^2-\Delta_0^2})\theta(|E|-\Delta_0)\ , \quad (7b)$$

and with a d-wave gap function,[18]

$$g_s^d(E)=\frac{2}{\pi^2 E}\begin{cases} K(k), & E>\dfrac{\Delta_0}{\sqrt{1+(\Delta_0/4t)^2}} \\ \dfrac{2}{\sqrt{k}}K(1/k), & E<\dfrac{\Delta_0}{\sqrt{1+(\Delta_0/4t)^2}} \end{cases}, \quad (7c)$$

where

$$k=\frac{[(4t)^2-E^2](\Delta_0^2-E^2)}{E^4}$$

and

$$K(x)\equiv\int_0^{\pi/2}d\theta\frac{1}{\sqrt{1-x\sin^2\theta}}$$

is the complete elliptic integral of the first kind. In the d-wave case, there is no gap in the superconducting case, although, clearly, states have been pushed into a logarithmic singularity. The singularity occurs at an energy $E=\Delta_0/\sqrt{1+(\Delta_0/4t)^2}$. In the s-wave case there is of course a gap at $E=\Delta_0$, with the usual square-root singularity. The result of the removal of states at low energy will turn out to be qualitatively similar: Fewer electron states will cause the phonon lifetimes to increase considerably. At energies beyond Δ_0, however, it turns out that a qualitative difference arises, as will be seen in the next section. In the normal state, scaling properties of the random-phase-approximation (RPA) susceptibility have been discussed recently by Ruvalds *et al.*[10] Of particular importance here is the result for the nesting wave vector, $\mathbf{q}=\mathbf{Q}[\equiv(\pi,\pi)]$, where the imaginary part of $\chi(\mathbf{Q},\nu+i\delta)$ is given analytically:[10]

$$-\mathrm{Im}\chi(\mathbf{Q},\nu+i\delta)=\frac{\pi}{2}g_n\left[\frac{\nu}{2}\right]\left[\tanh\left[\frac{\nu-2\mu}{4T}\right]+\tanh\left[\frac{\nu+2\mu}{4T}\right]\right]. \quad (8)$$

At low temperatures there is then a gap, $\nu_g=4|\mu|$, centered about zero frequency. This arises because the wave vector is constrained to be $\mathbf{Q}=(\pi,\pi)$, which, in the absence of impurities, can conserve energy only if the hole is at least $2|\mu|$ above the Fermi surface, which requires $|\nu|>2|\mu|$.

In Fig. 2 we show $-\mathrm{Im}\chi(q,\nu)$ for $q_x,q_y>0$ [note: $\chi(\pm q_x,\pm q_y,\nu)=\chi(q_x,q_y,\nu)$] for $\nu=0.5t$, and (a) $\mu=0.0$ (half-filling) and (b) $\mu=-0.8t$ at a low temperature ($T=0.01t$). The nesting feature present at half-filling manifests itself in the peak present at (π,π). This nesting transition is clearer in Fig. 3, where we show the energy

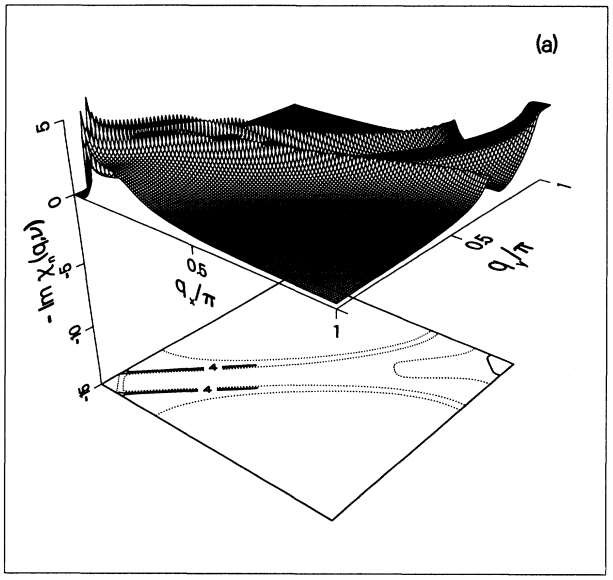

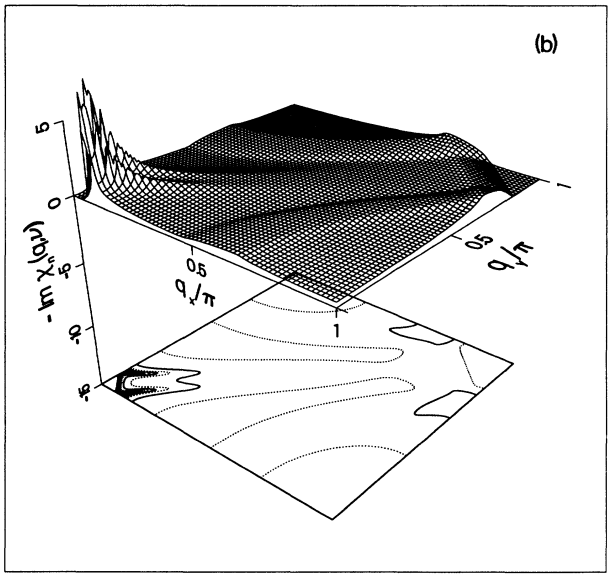

FIG. 2. $-\mathrm{Im}\chi(\mathbf{q},\nu+i\delta)$ vs $\mathbf{q}$ in the normal state for (a) $\mu=0$ (half-filling), and (b) $\mu=-0.8t$. We used $\nu=0.5t$ and essentially zero temperature. Note the peak at (π,π) in (a) where the Fermi surface is nested with nesting wave vector $\mathbf{Q}=(\pi,\pi)$.

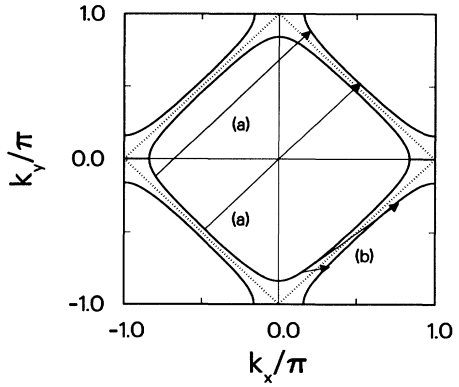

FIG. 3. Energy contours in the Brillouin zone. Momentum transfers of the kind labeled (a) in the figure give rise to the peak at (π,π) seen in Fig. 2(a). Momentum transfers of the kind labeled (b) give rise to the ridges shown in Fig. 2(a).

contours for $\epsilon_k = -0.25t$, 0, and $0.25t$. With $\nu = 0.5t$, the wave vectors of type (a) indicated in the figure connect states from below the Fermi surface ($\epsilon_k = 0$) to states above the Fermi surface with the desired energy difference ($\nu = 0.5t$). There are many of these, hence the peaks at $(\pm\pi, \pm\pi)$. The momenta vectors of type (b) (along with their Umklapp counterparts) give the ridges which occur alongside the diagonals. Note that along the diagonals there is a valley; it is essentially impossible to satisfy energy conservation with such momenta transfers. In Fig. 2(b) we show the corresponding result for $\mu = -0.8t$. The most noteworthy feature is the lack of a peak at $\mathbf{q} = (\pi, \pi)$ due to the lack of nesting. Note that in both cases there is always a gap at wave vectors near zero, since the energy difference associated which changes in electron states connected by such a small wave vector is insufficient to give the energy, $\nu (= 0.5t)$ in this case. Nonetheless, beyond this threshold there is always a peak, reflecting the fact that there is a large phase space for these transitions.

III. RESULTS IN THE SUPERCONDUCTING STATE

A. q dependence

In Fig. 4 we show $-\mathrm{Im}\chi(\mathbf{q}, \nu + i\delta)$ vs $\mathbf{q}$ in (a) the normal state, (b) the superconducting state with s-wave sym-

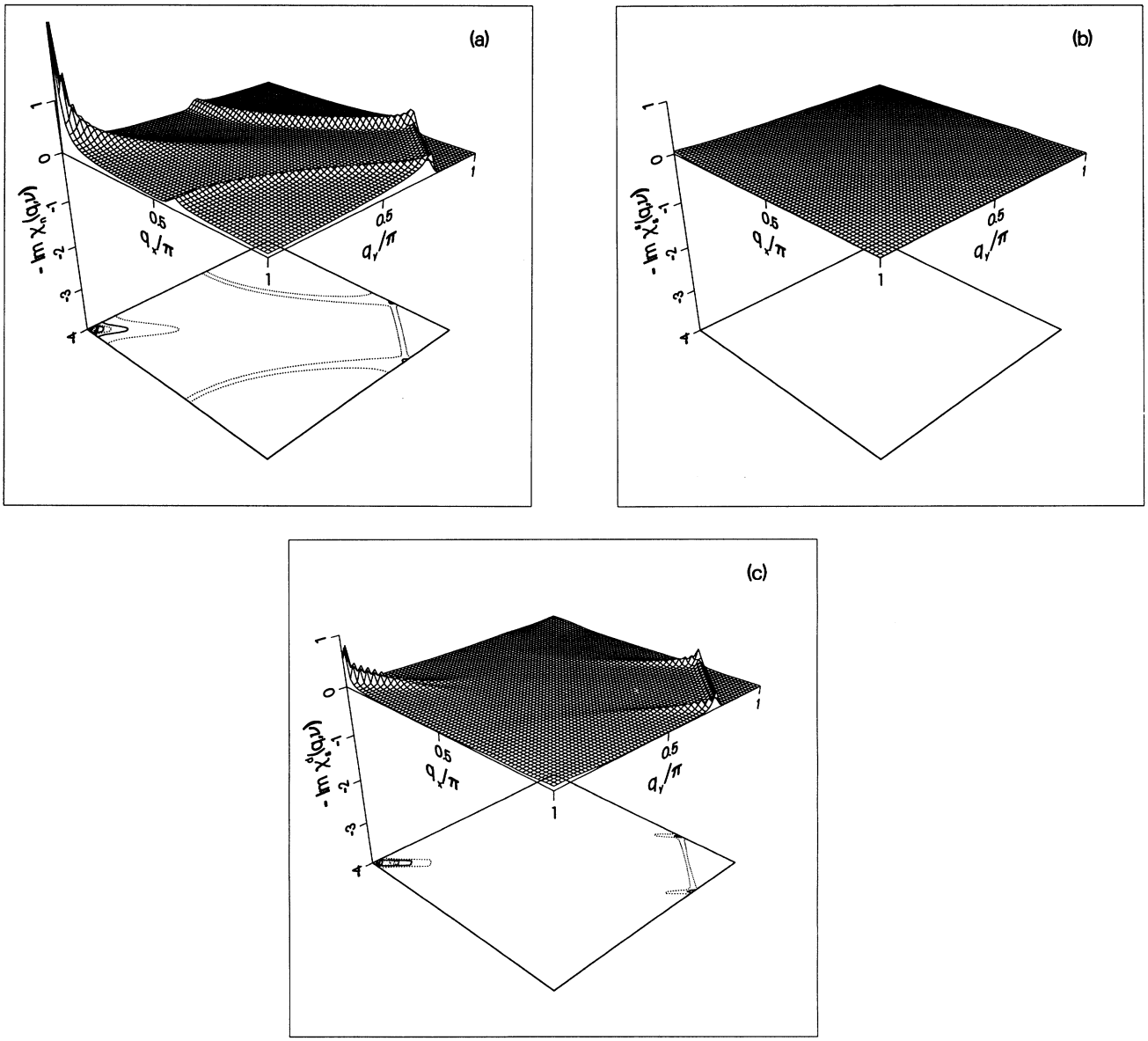

FIG. 4. $-\mathrm{Im}\chi(\mathbf{q}, \nu + i\delta)$ vs $\mathbf{q}$ in (a) the normal state, (b) the s-wave superconducting state, and (c) the d-wave superconducting state. The parameters used are $\mu = -0.8t$, $\nu = 0.1t$, $\Delta_0 = 0.2t$, and $T = 0.01t$. Note the complete suppression of $-\mathrm{Im}\chi(\mathbf{q}, \nu + i\delta)$ in the s-wave state, while remnants of the Fermi surface (where nodes in the gap function occur) remain the d-wave state.

metry, and (c) the superconducting state with d-wave symmetry. In all cases, we have used $\mu=-0.8t$, $v=0.1t$, $\Delta_0=0.2t$, $\delta=0.025t$, and $T=0.01t$. We have used the same scale in all three figures; $-\mathrm{Im}\chi(\mathbf{q},\nu+i\delta)$ is given in units of $1/8t$, so t is left arbitrary. It is immediately clear that, since $\nu<2\Delta_0$, the superconducting state with s-wave symmetry, which has produced a gap around the Fermi surface (see Fig. 1), has led to a complete suppression of $-\mathrm{Im}\chi(\mathbf{q},\nu+i\delta)$. Keeping in mind that the phonon lifetime is inversely proportional to this quantity, it is clear that the phonon lifetime (as attributed to the electron-phonon interaction, i.e., not including anharmonic effects, for example) has become essentially infinite. In the d-wave case, the situation is quite different, and peaks remain in $-\mathrm{Im}\chi(\mathbf{q},\nu+i\delta)$ due to the nodes in the gap function. For lower phonon frequency, the effect is even more pronounced as has been discussed for the NMR relaxation rate by Scalapino[19] and neutron-electron scattering by Lu.[20] The changes in the real part of the phonon self-energy indicate whether or not modes are expected to soften or harden. In Fig. 5 we plot $\mathrm{Re}[\chi_n(\mathbf{q},\nu+i\delta)-\chi_s^x(\mathbf{q},\nu+i\delta)]$ vs $\mathbf{q}$ for the same parameters as in Fig. 4. Here the subscript $n\,(s)$ means normal (superconducting) while the superscript $x=s$ or d, depending on

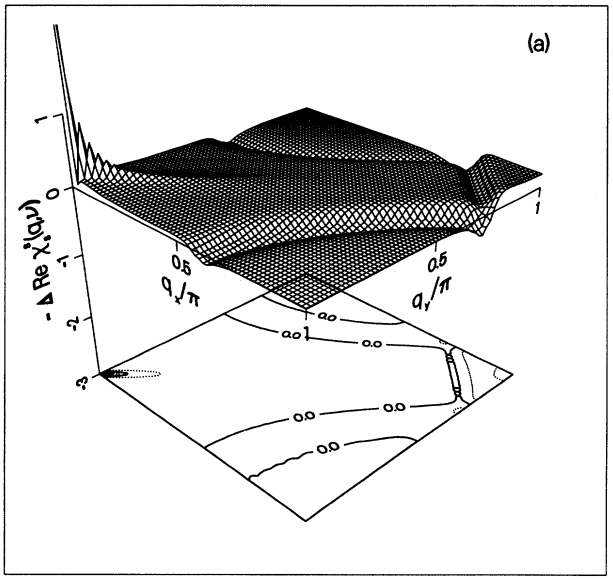

FIG. 5. Change in the real part of the susceptibility, $-\Delta\,\mathrm{Re}\chi(\mathbf{q},\nu+i\delta)=-\mathrm{Re}[\chi_s^x(\mathbf{q},\nu+i\delta)-\chi_n(\mathbf{q},\nu+i\delta)]$, (a) for s-wave superconductivity and (b) d-wave superconductivity. A positive (negative) result represents phonon softening (hardening). The parameters are as in Fig. 4.

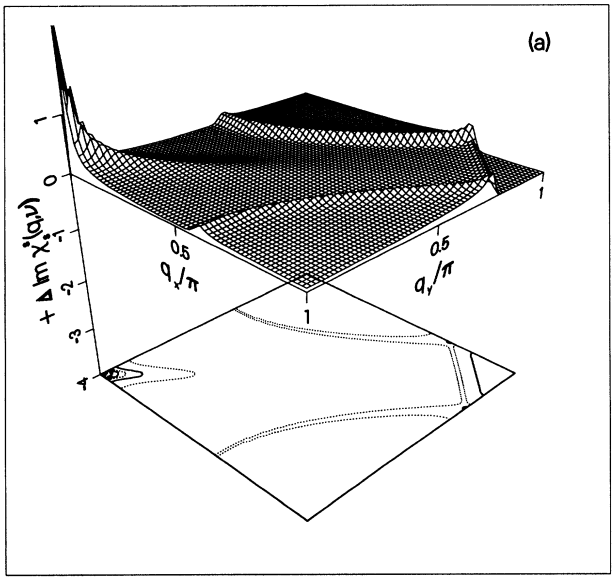

FIG. 6. Change in the imaginary part of the susceptibility $\{\Delta\,\mathrm{Im}\chi(\mathbf{q},\nu+i\delta)\equiv[\mathrm{Im}\chi_s^x(\mathbf{q},\nu+i\delta)]-[\mathrm{Im}\chi_n(\mathbf{q},\nu+i\delta)]\}$ vs $\mathbf{q}$ for (a) s-wave superconductivity, and (b) d-wave superconductivity. Here, a *positive* result represents phonon *narrowing* in the superconducting state. The parameters are as in Fig. 4.

the symmetry of the gap function. In Figs. 5(a) and 5(b) we show the results for a gap function of s-type and d-type symmetry, respectively. A positive result indicates a softening in the superconducting state relative to the normal state. The most pronounced hardening occurs at wave vectors almost connecting different parts of the Fermi surface, as discussed earlier. Hence the troughs, particularly visible in Fig. 5(a), follow the ridges seen earlier [Fig. 4(a)]. Overall, there is more hardening at large wave vectors in the case with d-wave symmetry [Fig. 5(b)]. In Fig. 6(a) we show the corresponding results for the difference of the imaginary parts:

$$\mathrm{Im}[\chi_s^x(\mathbf{q},\nu+i\delta)-\chi_n(\mathbf{q},\nu+i\delta)]\ ,$$

where it is clear that in both cases the phonons narrow in the superconducting state (positive difference).

The situation for higher-frequency phonons is, of course, very different. In Figs. 7(a) and 7(b) we plot the difference in $\mathrm{Im}\chi(\mathbf{q},\nu+i\delta)$ for $\nu=1.8t$. We find that the momentum space over which narrowing occurs is highly restricted in the s-wave case, to lie along the ridges already alluded to earlier. In the d-wave case the regime over which narrowing occurs is much greater. This is as expected, since the reason for the broadening in the su-

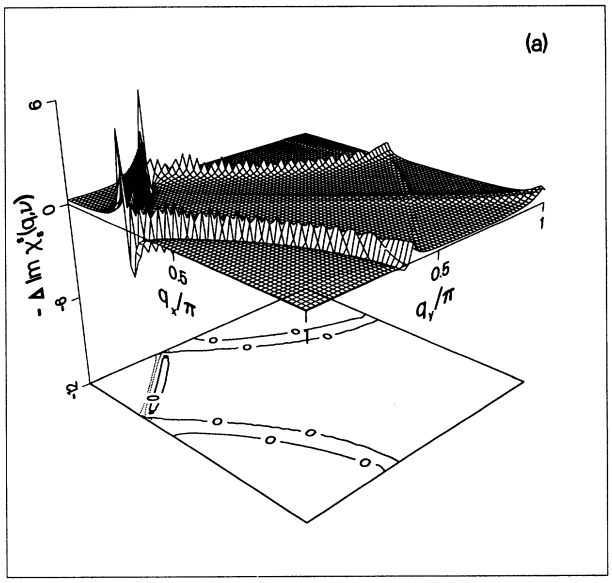

FIG. 7. *Negative* change in the imaginary part of the susceptibility, $-\Delta\,\mathrm{Im}\chi(\mathbf{q},\nu+i\delta)$, vs $\mathbf{q}$ for (a) s-wave superconductivity, and (b) d-wave superconductivity, for the same parameters as in Fig. 4, except that the frequency is higher, $\nu=1.8t$. Here a *positive* result represents phonon *broadening*.

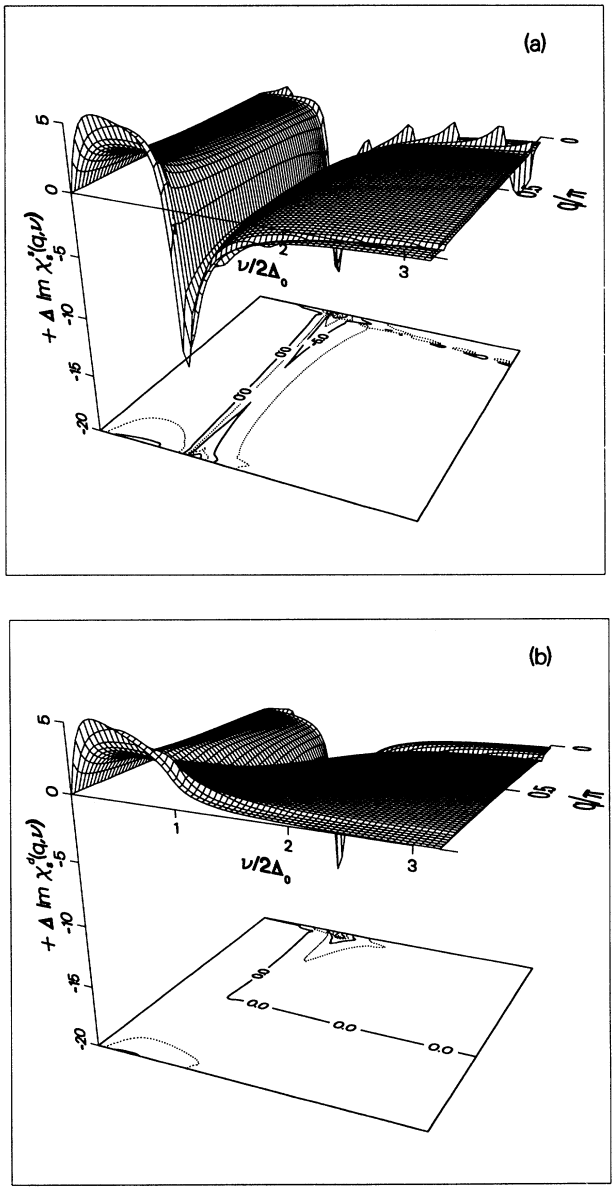

FIG. 8. Change in the imaginary part of the susceptibility vs frequency and q, where $\mathbf{q}=(q,q)$ for (a) s-wave superconductivity, and (b) d-wave superconductivity, for $\mu=0$, $\Delta_0=0.2t$, and $T=0.01t$. A positive result represents narrowing. Note that no broadening occurs near $\mathbf{q}=(\pi,\pi)$ in the d-wave case.

perconducting state is the increased single-particle density of states for frequencies $\nu > \Delta_0$. However the increase in the density of states is much greater for an s-wave gap function (square-root singularity) than for a d-wave gap function (logarithmic singularity). The fact that phonon narrowing is even possible for frequencies above the gap is more easily seen in the case of an s-wave gap function [Fig. 7(a)], where the wave vectors for phonon narrowing are confined to two narrow ridges. It turns out that the phonon linewidths in the normal state are enhanced, just as they were for lower frequency [see Fig. 4(a)]. In the superconducting state, however, one can simply no longer satisfy both momentum and energy conservation, so that the phonon line shapes will narrow, in spite of the enhanced single-particle density of states.

B. Frequency dependence

To examine more closely the frequency dependence of the changes in phonon self-energy, we take slices in the (q_x, q_y) plane and plot specifically the change in $\mathrm{Im}\chi(\mathbf{q}, \nu + i\delta)$,

$$\Delta\,\mathrm{Im}\chi(\mathbf{q}, \nu + i\delta) = [\mathrm{Im}\chi_s^x(\mathbf{q}, \nu + i\delta)] - [\mathrm{Im}\chi_n(\mathbf{q}, \nu + i\delta)] \ ,$$

for $x \equiv s$ or d. In Fig. 8 we show $\Delta\,\mathrm{Im}\chi(\mathbf{q}, \nu + i\delta)$ vs ν, for $\mathbf{q}$ along the diagonal, $\mathbf{q} = (q, q)$, with $\Delta_0 = 0.2t$, $\mu = 0$, $T = 0.01t$, and $\delta = 0.025t$, for (a) an s-wave gap function, and (b) a d-wave gap function. Note that for $\nu < 2\Delta_0$, in both cases there is a phonon narrowing upon entering the superconducting state [$\Delta\,\mathrm{Im}\chi(\mathbf{q}, \nu + i\delta) > 0$]. Actually, for $\mathbf{q} \approx (0,0)$ there is in fact no narrowing, which is most evident if one examines the contours plotted below the figures. In the s-wave case this is in agreement with previous calculations.[6,7] To clarify the situation at $\mathbf{q} = 0$ we show in Fig. 9(a) $\Delta\,\mathrm{Im}\chi(\mathbf{q} = 0, \nu + i\delta)$ vs $\nu/2\Delta_0$ for both the s-wave and d-wave cases. These results are given analytically by

$$-\mathrm{Im}\chi_s^x(\mathbf{q} = 0, \nu + i\delta) = \pi \left[\frac{2\Delta_0}{\nu} \right]^2 \bar{g}_s^x \left[\frac{\nu}{2} \right] \tanh \frac{\beta\nu}{4} \ , \qquad (9)$$

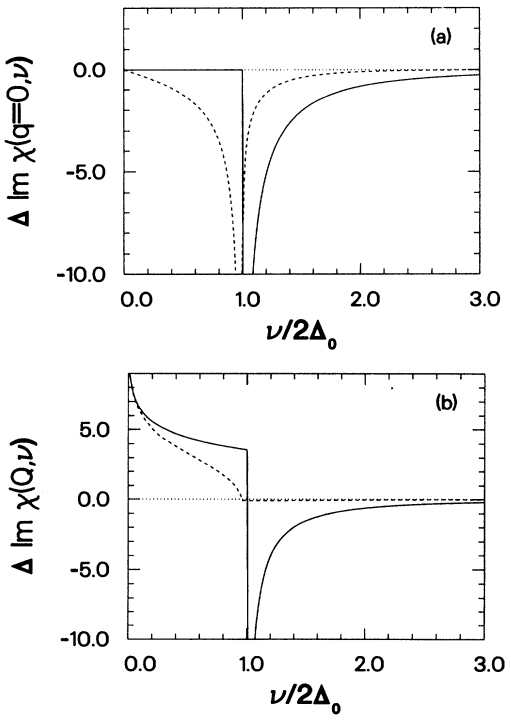

FIG. 9. $\Delta\,\mathrm{Im}\chi(\mathbf{q} = 0, \nu + i\delta)$ vs $\nu/2\Delta_0$ for (a) $\mathbf{q} = 0$, and (b) $\mathbf{q} = (\pi, \pi)$, for the parameters of Fig. 8. The s-wave (d-wave) result is given by the solid (dashed) curve. A positive result represents narrowing of the phonon line shape.

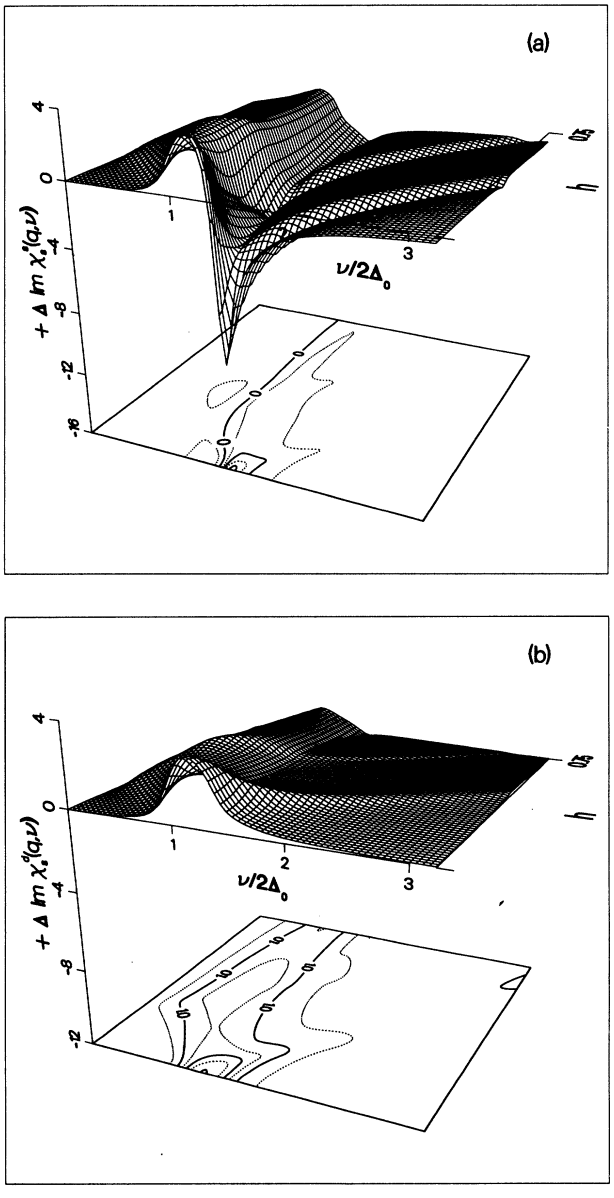

FIG. 10. $\Delta\,\mathrm{Im}\chi(\mathbf{q}, \nu + i\delta)$ vs $\nu/2\Delta_0$ and h, where $\mathbf{q} = (\pi, h\pi)$, and $\frac{3}{4} \le h \le 1$ for (a) s-wave superconductivity, and (b) d-wave superconductivity, for $\mu = -0.2t$, $\Delta_0 = 0.2t$, and $T = 0.01t$. A positive result represents phonon narrowing.

where $\bar{g}_s^s(E) \equiv g_s^s(E)$ and

$$\bar{g}_s^d(E) \equiv \frac{1}{N} \sum_k \left[\frac{\Delta_k}{\Delta_0} \right]^2 \left[\frac{\delta(E-E_k)+\delta(E+E_k)}{2} \right], \quad (10)$$

which can be evaluated in terms of complete elliptic integrals of the first and third kind. In both cases only broadening occurs; the difference is that for frequencies $\nu < 2\Delta_0$, there is no change in the s-wave case, while broadening occurs in the d-wave case.

Returning to Fig. 8, we note that the situation for frequencies $\nu > 2\Delta_0$ is significantly different in the two cases shown, for $\mathbf{q} \approx \mathbf{Q}[\equiv(\pi,\pi)]$. Specifically, in the s-wave case a significant broadening occurs for $\nu > 2\Delta_0$, whereas in the d-wave case the phonons become narrower in the superconducting state at all frequencies. The results are again obtained analytically at half-filling for $\mathbf{q}=\mathbf{Q}=(\pi,\pi)$:

$$-\mathrm{Im}\chi_s^s(\mathbf{Q},\nu+i\delta) = \pi g_s^s \left[\frac{\nu}{2} \right] \tanh \frac{\beta\nu}{4} \quad s \text{ wave}, \quad (11a)$$

$$-\mathrm{Im}\chi_s^d(\mathbf{Q},\nu+i\delta) = \pi \left[g_s^d \left[\frac{\nu}{2} \right] - \left[\frac{2\Delta_0}{\nu} \right]^2 \bar{g}_s^d \left[\frac{\nu}{2} \right] \right] \times \tanh \frac{\beta\nu}{4} \quad d \text{ wave}, \quad (11b)$$

and are plotted in Fig. 9(b).

What changes occur as we dope away from half-filling? In Fig. 10 we focus on the region near (π,π) and plot $\Delta\,\mathrm{Im}\chi(q,\nu+i\delta)$ vs $\nu/2\Delta_0$ along the zone edge $\mathbf{q}=(\pi,h\pi)$, $\frac{3}{4} \le h \le 1$, with the chemical potential $\mu=-0.2t$, for (a) an s-wave, and (b) a d-wave gap function. We note that very close to $\mathbf{q}=(\pi,\pi)$ there is no change in the phonon lifetime at very low frequency. This is due to the fact that there is no scattering in both the superconducting and normal state at frequencies $\nu \le 2|\mu|$ [see Eq. (8)]. For $2|\mu| \le \nu \le 2\sqrt{|\mu|^2+\Delta_0^2}$, phonons can decay in the normal state, but not in the superconducting state, for the same reasons as in Fig. 8. Finally for $\nu > 2\sqrt{|\mu|^2+\Delta_0^2}$, phonons broaden significantly in the s-wave case, while little change occurs in the d-wave case.

C. Dependence on chemical potential

To see the dependence on chemical potential in more detail, we fix $\mathbf{q}=(\pi,\pi)$ and plot $\Delta\,\mathrm{Im}\chi(\mathbf{q},\nu+i\delta)$ vs $\nu/2\Delta_0$ while varying the chemical potential. In Fig. 11(a) we show the s-wave case. At $\mu=0$ in particular, we see the narrowing for $\nu < 2\Delta_0$, followed by broadening for $\nu > 2\Delta_0$. The effect of increasing $|\mu|$ is more clearly seen in Fig. 11(b) where we show a rear view of the same figure. Clearly, for nonzero $|\mu|$, there is a low-frequency regime in which no phonon self-energy change occurs, followed by a frequency regime where narrowing would occur, followed by another where broadening occurs. From an experimental point of view, one can imagine monitoring a phonon whose frequency is above $2\Delta_0$, and assumed fixed as a function of doping. Then, very close to half-filling, the phonon will experience a significant broadening in the superconducting state. Upon further doping, the phonon will actually narrow, followed eventually by a regime where no change will occur. In Fig. 12 we show the same result (front view only) for a d-wave gap function. No broadening is now present but the phonon linewidth experiences similar nonmonotonic changes as a function of doping.

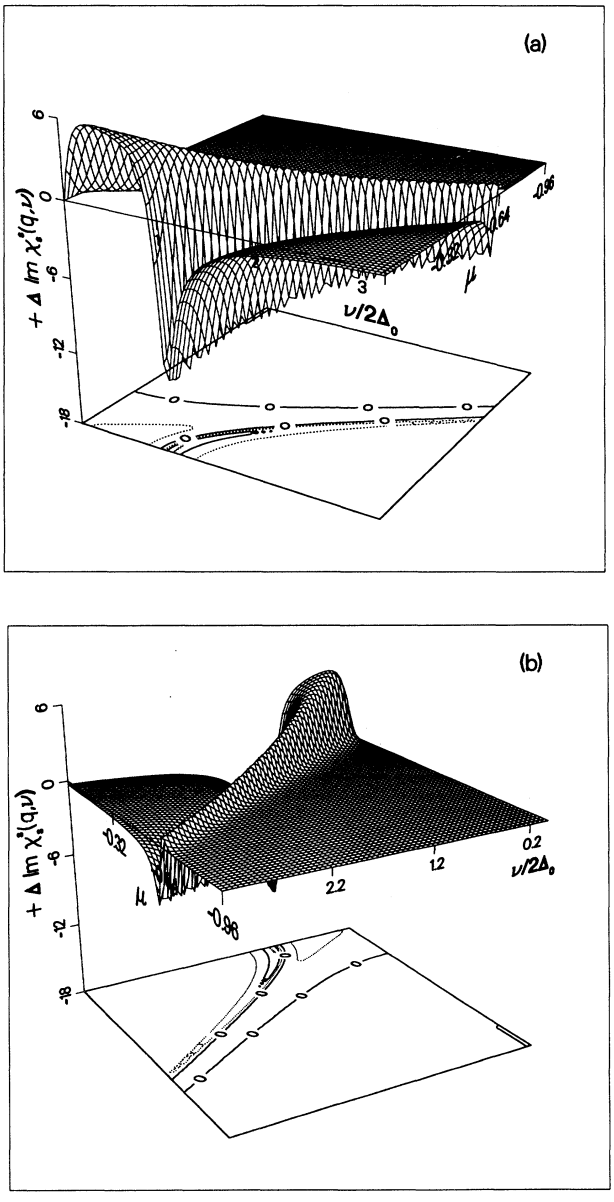

FIG. 11. (a) "Front" view and (b) "rear" view of $\Delta\,\mathrm{Im}\chi(\mathbf{q},\nu+i\delta)$ vs $\nu/2\Delta_0$ and μ in the s-wave superconducting state. We used $\mathbf{q}=(\pi,\pi)$, $\Delta_0=0.2t$, and $T=0.01t$. Note that the change in phonon linewidth (with fixed frequency) can change sign as a function of doping (increasing $|\mu|$). A positive result represents phonon narrowing.

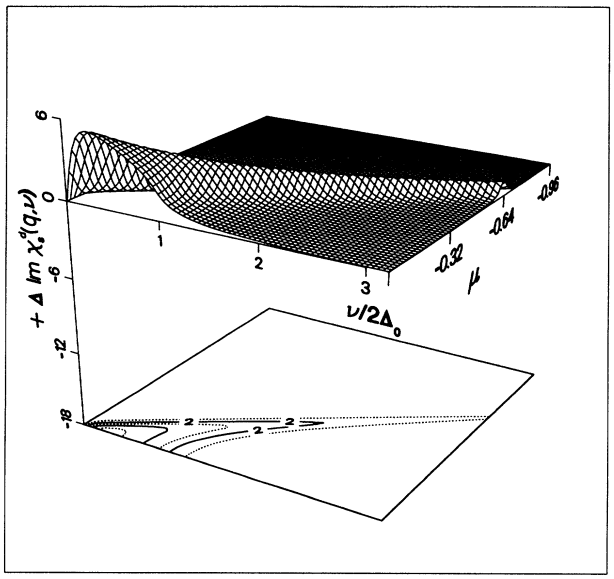

FIG. 12. $\Delta\,\mathrm{Im}\chi(\mathbf{q},\nu+i\delta)$ vs $\nu/2\Delta_0$ and μ in the d-wave superconducting state, with the same parameters as in Fig. 11. A positive result represents phonon narrowing.

IV. SUMMARY

We have investigated the variety of possible changes phonons could undergo as a material goes superconducting, with a gap function of either s-wave or d-wave type symmetry. It is generally true that as electron states are removed close to the Fermi level, less phase space for phonon decay through quasiparticle scattering is available, so that low-frequency phonon lifetimes will generally increase. Whether or not softening or hardening of the phonon frequency accompanies this lifetime increase depends on the wave vector of the phonon involved. For higher-frequency phonons, there is a qualitative difference in the phonon lifetime behavior, depending on the gap function symmetry, and also depending on the wave vectors involved. Even for the s-wave case, where the single-particle density of states has a strong square-root singularity above the single-particle gap, there exist wave vectors at which a high-frequency phonon would narrow, simply because momentum and energy could not be conserved in the superconducting state.

We should emphasize that we have used a simple tight-binding band structure, which is nested at half-filling, to present some of the features expected from a nested or nearly-nested band structure. In particular, the nonmonotonic behavior of the phonon lifetime change as a function of doping, for a nearly-nested wave vector, would be a clear signature of some nesting phenomenon.

It is of course impossible to exhaust all possibilities and to explore all parameter space within such a model. In the present paper we have focused on particular parameter regimes where interesting effects arise, which, at the same time, may be relevant to experiments. We have not, however, tried to make detailed predictions, nor, for example, have we even varied the band structure to give more realistic models. In this connection we wish to encourage further inelastic-neutron-scattering experiments of the type first carried out by Axe and Shirane,[12] particularly for $YBa_2Cu_3O_{7-\delta}$. Through careful experimental studies of phonons throughout the Brillouin zone, along with theoretical analysis of the kind presented in this paper, it is possible that definitive answers regarding gap symmetry and Fermi-surface topology can be provided.

[1]See, for example, *Lattice Effects in High-T_c Superconductors*, edited by T. Egami, Y. Bar-Yam, J. Mustre-de Leon, and A. Bishop (World Scientific, Singapore, 1992).
[2]B. Friedl, C. Thomsen, and M. Cardona, Phys. Rev. Lett. **65**, 915 (1990).
[3]H. A. Mook, M. Mostoller, J. A. Harvey, N. W. Hill, B. C. Chakoumakos, and B. C. Sales, Phys. Rev. Lett. **65**, 2712 (1990).
[4]Thomas Timusk, C. D. Porter, and D. B. Tanner, Phys. Rev. Lett. **66**, 663 (1991).
[5]R. P. Sharma, L. E. Rehn, P. M. Baldo, and J. Z. Liu, Phys. Rev. Lett. **62**, 2869 (1989).
[6]R. Zeyher and G. Zwicknagl, Solid State Commun. **66**, 617 (1988); Z. Phys. B **78**, 175 (1990).
[7]F. Marsiglio, R. Akis, and J. P. Carbotte, Phys. Rev. B **45**, 9865 (1992).
[8]E. Altendorf, J. C. Irwin, R. Liang, and W. N. Hardy, Phys. Rev. B **45**, 7551 (1992).
[9]R. Zeyher, Phys. Rev. B **44**, 9596 (1991).
[10]J. Ruvalds, C. T. Rieck, J. Zhang, and A. Virosztek, Science **256**, 1664 (1992).
[11]See, for example, articles in *High Temperature Superconductivity*, Los Alamos Symposium, edited by K. S. Bedell *et al.* (Addison-Wesley, Don Mills, 1990).
[12]J. D. Axe and G. Shirane, Phys. Rev. Lett. **30**, 214 (1973); S. M. Shapiro, G. Shirane, and J. D. Axe, Phys. Rev. **12**, 4899 (1975).
[13]Henry Chou, K. Yamada, J. D. Axe, S. M. Shapiro, G. Shirane, Isao Tanaka, Kenichi Yamane, and Hironao Kojima, Phys. Rev. B **42**, 4272 (1990).
[14]W. Reichardt (private communication).
[15]F. Marsiglio, in Ref. 1.
[16]M. E. Flatté (unpublished).
[17]J. E. Hirsch and F. Marsiglio, Phys. Rev. B **39**, 11 515 (1989).
[18]C. Zhou and H. J. Schulz, Phys. Rev. B **45**, 7397 (1992).
[19]D. J. Scalapino, in Ref. 11, p. 400.
[20]J. P. Lu, Phys. Rev. Lett. **68**, 125 (1992).